Dielectric profiling of Enceladus' surface in the Tiger Stripe Region P. Friend[1] and A. Kyriacou[1], [1]University of Wuppertal, Department of Physics, Gaussstrasse 20, 42119 Wuppertal, Germany, friend@uni-wuppertal.de , kyriacou@uni-wuppertal.de

Introduction: Saturn's icy moon Enceladus is among the most promising candidates in our solar system to host extraterrestrial life. A mission proposal addressing this question, Enceladus Explorer, includes a melting probe that descends in close vicinity of the tiger stripes to probe a near surface water reservoir which is supplied from the cryo-volcanism. Orbital radar could be used to map the landing area from the orbit, to image the subsurface and locate such a water pocket. After landing, an ice-penetrating radar based from the surface and from within the ice can be used to improve localization of the target reservoir and help navigate the melting probe [1]. To accurately determine the depth and position of the aquifer, the dielectric properties of the intervening ice must be understood. This is given by the real part of the dielectric constant/permittivity (ε_r) and depends on the physical and chemical properties of the ice. Enceladus' surface is made overwhelmingly of pure water ice (99%) [2], with the Tiger Stripe region likely covered in a layer of deposited ice grains, originating from active geysers, leading to a surface with high porosity of ~0.9 [3] and a density of ρ = 92 kg/m^3. In close vicinity to the Tiger Stripes, these deposits are also subject to sintering due to the higher heat flux. As such, the mechanical, thermal and dielectric properties of the ice between the surface and possible subsurface aquifers cannot be assumed to be homogenous. An analysis of surface temperatures, grain deposition rate and topography is to be conducted to calculate the dielectric profile of the upper ~100 metres of Enceladus' south polar terrain. A first step, which is provided here, is to estimate the depth and density profile of the deposited ice grains originating from the south polar geysers.

Methods: Over 207 active cryovolcanoes/geysers have been identified on Enceladus, including 6 hotspots proposed by [4] and 115 weaker sources distinguished by [5] and [6]. They are all associated with 4 parallel fractures along the south polar terrain known as the Tiger Stripes.

A previous work [7] did extensive modelling of the geyser plume eruptions, calculating collision rates of geyser particles with Enceladus' surface, for grain size ranges from 0.5 um to 15 um. The simulated data was stored in arrays of (180x360) with the position of the bins corresponding to a latitude and longitude coordinate, and the bin itself recording the rate of deposited ice grains in accumulated depth per unit time.

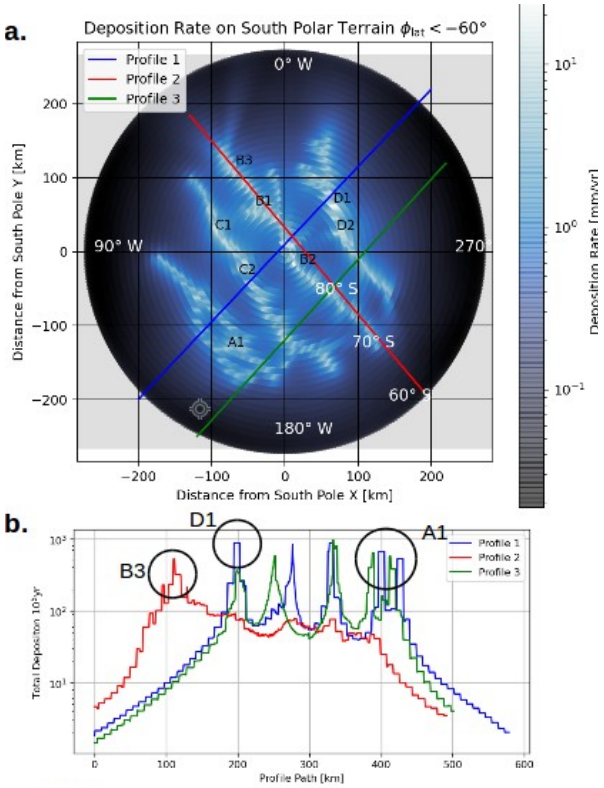

Figure 1:
a. An intensity map of geyser deposition rate [mm/yr] overlaying a polar stereographic mosaic of the South Polar terrain (60°S). 3 path profiles are shown (1,2 and 3) and the total deposition over 100,000 years is shown in **b.** The deposition rate is of order 1 mm/yr over the South Pole and reaches a maximum of 10 mm/yr above the designated hotspots (A1, B1, B2, B3, C1, C2, D1, D2).
Alexandria is shown in the bottom left, with Cairo, Baghdad and Damascus visible in order from bottom-left to top-right

b. The integrated deposition depth of 100,000 years is plotted over the path length over the surface for profiles 1, 2 and 3. Note that profile 1 passes over a known hotspot (D1).

From this data we plotted the two dimensional distribution of ice deposition from the plumes over the South Polar terrain (latitudes below 60 S, or up to 250 km away from the southern pole) in polar stereographic projection.

The deposition rate was then integrated over a range of time periods (from 10 kyr to 1 Myr) constrained by the surface age T < 1 Myr from crater counting [8]. We assume a constant total eruption rate over this time period of dM/dt =40 kg/s equaling the currently observed value in [7] .

Results: Figure 1a shows the surface ice deposition rate over the south polar region (latitudes < 60 S), for ice grains ranging from 0.5 microns < R <

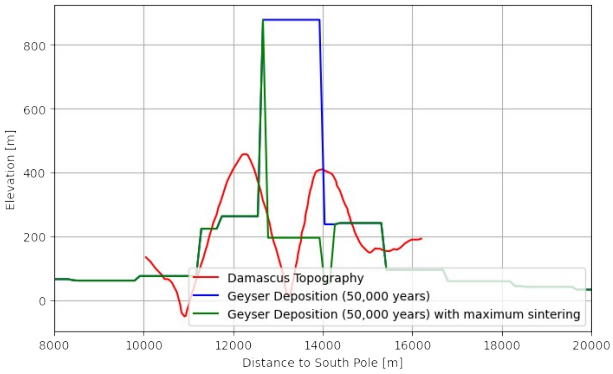

Figure 2
A comparison of the cross-sectional topography of Damascus Sulcus (mapped by Cassini in August 2008 [3]) with the predicted ice deposition over 50,000 years at the position of hotspot D1 and maximum densification due to ice grain sintering.

15 microns.. The regions of highest intensity of deposition (at ~ 10 mm/yr) closely matches with the positions of the Tiger Stripes. In the surrounding terrain at (< 80 S) the mean deposition rate is ~1 mm/yr. Directly inside the Tiger Stripes ridges, the surface temperature reaches 180-200 K, where sintering would occur on a timescale of minutes, but the temperature falls rapidly with lateral distance, down to 80 K after 1000 m, at which sintering will not occur within the lifetime of the solar system [9]. It is noteworthy that the deposition rate and temperature fall on a similar distance scale.

Figure 1b shows 3 profiles which are plotted along Fig. 1a over representative paths at the South Polar terrain. Profile 1 cuts through all 4 Tiger Stripes,the South Pole and the hotspot D1 in Damascus Sulcus. Profile 2 runs roughly parallel with Baghdad Sulcus. Profile 3 runs parallel to Profile 1 with an offset by a radial distance of 140 km and intercepts also with all 4 Tiger Stripes. The 6 known hotpots are clearly visible in these profiles.

Figure 2 compares the topography of Damascus sulcus as observed by Cassini during its August 2008 flyby [3] with the predicted thickness of the ice grain deposition assuming a constant output since 100 kyr. Assuming also a maximum compaction of the deposits from sintering (with a porosity decrease from 0.9 to 0.2) inside the Tiger Stripes, we find that the resulting thickness of the ice grain deposits are in good agreement with the observed topography. However, higher resolution maps of the surface temperature in this region are necessary for robust calculations of the sintering and resulting densification rate. Also, data on the densification rate due to sintering will yet need to be implemented into the model.

Conclusion: The position of the deepest plume deposits correlates with CIRS observations of recently formed crystalline ice [10] most probably formed from sintering processes and the location of highest heat flux [11]. We further find that the topography of Damascus sulcus places a limit on the active life time of the Tiger Stripe region to less than 100,000 years, and in this case of a hotspot D1 the time of activity is no more than 50,000 years. Hence, single hot spots have likely changed their location within the active time of the Tiger Stripes. From our data, we further expect that the south polar region (latitude less than -80 degrees) is covered in a layer of unconsolidated ice grains which has a thickness on the order of ~100 m. Such a layer should easily be distinguishable to orbital radar, with a refractive index of $n = 1.08$ ($\varepsilon_r = 1.149$ and $v_{radar} = 280$ m/us) in the GHz range and must be taken into account in orbital searches for aquifers

Acknowledgments: The ice deposition data was provided in HDF5 files, available via: http://impact.colorado.edu/southworth_data, kindly made available from [4].

We thank the German Aerospace Centre (DLR-Raumfahrtmanagement) for funding the Enceladus Explorer (EnEx) initiative and EnEx-AsGAr under the project number 50 NA 1709 .

References: [1] Konstantinides K. et.al. (2015) *Acta Astronautica 106*, 33-89. [2] Postberg F. et al. (2018) in *Enceladus and the Icy Moons of Saturn*, 129-163. [3] Burrati B. J. et al. (2014) LPSC 45, 2038. [4] Spitale and Porco (2007) *Nature Letters 449*, 695-697. [5] Spitale J. et al. (2015) *Nature 521*, 57–60. [6] Porco et al. (2014) *The Astronomy Journal 148*, 45. [7] Southworth B. S. et al. (2019) *Icarus 319*, 33-42. [8] Porco C. et al. (2006) Science *311*, 1393-1401. [9] Gundlach B. et al. (2018) *Monthly Notices of the Royal Astronomical Society 479*, 5272-5287. [10] Robidel R. et al. (2010) *Icarus preprint* [11]Spitale J. et al. (2015) *Nature 521*, 57–60